Cellular Immunostimulation by CpG-Sequence-Coated DNA Origami Structures

Verena J. Schüller,[†,⊥] Simon Heidegger,[‡,⊥] Nadja Sandholzer,[‡] Philipp C. Nickels,[†] Nina A. Suhartha,[‡] Stefan Endres,[‡] Carole Bourquin,[‡,§,*] and Tim Liedl[†,*]

[†]Center for Nanoscience and Department of Physics, Ludwig-Maximilians-Universität, Geschwister-Scholl-Platz 1, 80539 München, Germany, [‡]Abteilung für Klinische Pharmakologie, Medizinische Klinik, Klinik der Universität München, Ziemssenstrasse 1, 80336 München, Germany, and [§]Chair of Pharmacology, Department of Medicine, University of Fribourg, Chemin du Musée 5, 1700 Fribourg, Switzerland. [⊥]These authors contributed equally to this work.

ABSTRACT To investigate the potential of DNA origami constructs as programmable and noncytotoxic immunostimulants, we tested the immune responses induced by hollow 30-helix DNA origami tubes covered with up to 62 cytosine-phosphate-guanine (CpG) sequences in freshly isolated spleen cells. Unmethylated CpG sequences that are highly specific for bacterial DNA are recognized by a specialized receptor of the innate immune system localized in the endosome, the Toll-like receptor 9 (TLR9). When incubated with oligonucleotides containing CpGs, immune cells are stimulated through TLR9 to produce and secrete cytokine mediators such as interleukin-6 (IL-6) and interleukin-12p70 (IL-12p70), a process associated with the initiation of an immune response. In our studies, the DNA origami tube built from an 8634 nt long variant of the commonly used single-stranded DNA origami scaffold M13mp18 and 227 staple oligonucleotides decorated with 62 CpG-containing oligonucleotides triggered a strong immune response, characterized by cytokine production and immune cell activation, which was entirely dependent on TLR9 stimulation. Such decorated origami tubes also triggered higher immunostimulation than equal amounts of CpG oligonucleotides associated with a standard carrier system such as Lipofectamine. In the absence of CpG oligonucleotides, cytokine production induced by the origami tubes was low and was not related to TLR9 recognition. Fluorescent microscopy revealed localization of CpG-containing DNA origami structures in the endosome. The DNA constructs showed in contrast to Lipofectamine no detectable toxicity and did not affect the viability of splenocytes. We thus demonstrate that DNA origami constructs represent a delivery system for CpG oligonucleotides that is both efficient and nontoxic.

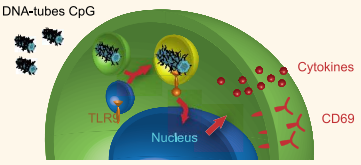

KEYWORDS: DNA origami · DNA nanotechnology · immunology · cytotoxicity · CpG

Rapid development of the field of DNA nanotechnology, where DNA is used as a building material for nanoscale objects[1,2] and functional devices,[3,4] opens the route for the construction of carrier systems that can interact with cellular machinery on the molecular level. In particular, DNA assemblies based on the DNA origami method[5−7] can exhibit shapes of high complexity presenting nanometer-precise arrangements of (biomolecular) components on their surfaces.[8−11] This method uses a 7 to 8 kb long M13mp18 phage-derived DNA single strand that is folded into a desired shape by some 200 oligonucleotides. To be employable as a molecular carrier system in mammals, any DNA construct must meet three important criteria: (i) it needs to be stable in the extracellular space and in the cytoplasm of the cell long enough to fulfill its predefined task; (ii) no toxic side effects should occur; and (iii) the mammalian immune system should tolerate the nanoscopic carrier systems. So far, it has been shown that oligonucleotide-based tetrahedral cages are resistant to several endonucleases,[12] can enter mammalian cells, stay intact, once taken up, for at least 48 h,[13] and can act as carriers of CpG oligonucleotides into macrophage-like RAW264.7 cells, as shown in a very recent study by Li *et al.*[14] Also Nishikawa, Takakura, and co-workers have demonstrated earlier that Y-shaped and dendritic CpG-containing DNA structures are internalized efficiently by the same cell line and provoke enhanced immunostimulation responses.[15,16] Furthermore, programmed RNA hairpins can sequence-selectively trigger apoptosis in cancer cells[17] or act as color-coded labels in *in situ* experiments[18] in a wide variety of cell types. A further study tested the degradation of DNA origami structures exposed to multiple endonucleases, including DNase I, T7 endonuclease I, T7 exonuclease, *Escherichia coli* exonuclease I, Lambda exonuclease, and MseI restriction endonuclease and found high stabilities of the DNA constructs compared to duplex plasmid DNA.[19] This is consistent with findings of Mei *et al.*, who demonstrated that DNA

* Address correspondence to carole.bourquin@unifr.ch, tim.liedl@lmu.de.

Received for review August 17, 2011 and accepted November 17, 2011.

Published online November 17, 2011
10.1021/nn203161y

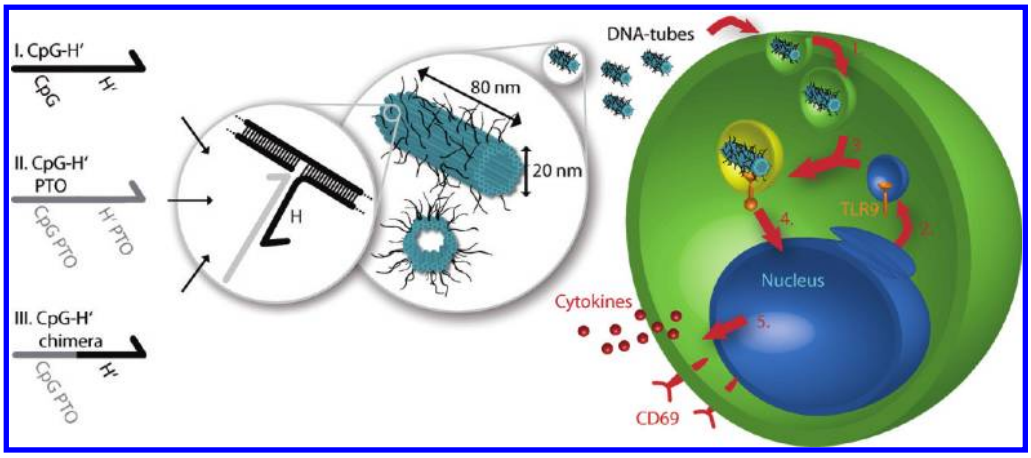

Scheme 1. Design of 30-helix DNA origami tube and endocytotic pathway. Left: Three different types of CpG-H′s with (I) unmodified phosphate backbone, (II) phosphorothioate (PTO)-modified backbone, and (III) partly PTO-modified backbone. Middle: Computer model of front (bottom) and side (top) view of 30-helix tube. Blue cylinders indicate double helices; black lines indicate possible connection sites for CpG sequences. Right: (1) DNA origami tube internalized by endocytosis; (2) vesicle segregated by the Golgi apparatus containing the transmembrane Toll-like receptor 9 (TLR9); (3) fusion of endosome with DNA origami tube and TLR9 containing vesicle; (4) recognition of CpG sequence by TLR9 and starting signaling cascade; (5) expression of surface molecules and release of cytokines that stimulate the further immune response.

origami structures maintain their structural integrity when exposed to cell lysates of various cell lines.[20]

In this study, we focused on the immunological response of mammalian primary splenic cells to DNA origami structures. Indeed, the mammalian immune system is poised to detect foreign DNA from invading viruses or bacteria through specific receptors that, upon recognition of their cognate DNA ligand, initiate a full-blown immune response. One such receptor is the endosomal Toll-like receptor 9 (TLR9), which recognizes unmethylated CpG sequences that are a hallmark of microbial DNA.[21] Further immunological DNA receptors detect DNA structures from viruses in the cytosol, from which endogenous DNA is normally absent.[22] Stimulation of these receptors following specific recognition of DNA leads to activation of innate immunity and, in particular, to the secretion of proinflammatory cytokine mediators such as the interleukinsIL-6 and IL-12p70.[23,24] For the implementation of DNA origami constructs as molecular delivery systems, it is therefore essential to fully understand their immunostimulatory potential in order to tightly control the initiation of immune responses according to the therapeutic goal.

RESULTS AND DISCUSSION

We designed a DNA origami construct to serve as an efficient biologically active carrier system for CpG sequences in order to stimulate immune responses in mammalian cells. For this purpose, we developed a hollow tube-shaped DNA origami structure consisting of 30 parallel double helices with maximized surface area for both 62 inner or 62 outer binding sites (handle sequences H) for cytosine-phosphate-guanine (CpG) + anchor sequences (CpG-H′s). The CpG sequence used in all experiments is referred to as CpG 1826, a well-characterized, highly active 20-mer oligonucleotide, which is specific for mouse TLR9.[25] Three different types of phosphate backbone for the CpG-H′s were used in this study: (I) unmodified CpG-H′ (tube CpG); (II) CpG-H′ PTO with a phosphorothioate-modified backbone (tube CpG PTO); (III) CpG-H′ chimera with PTO-modified CpG sequence and unmodified H′ sequence (tube chimera)(see Materials and Methods). A plain tube without handles H for CpG-H′s (tube w/o CpG) as well as tubes decorated with GpC-H′s instead of CpG-H′s served as controls. The DNA origami tubes were assembled from 227 oligonucleotides (staple strands) that fold an 8634 nucleotide (nt) M13mp18-based single strand (scaffold) into shape during a 2 h long annealing

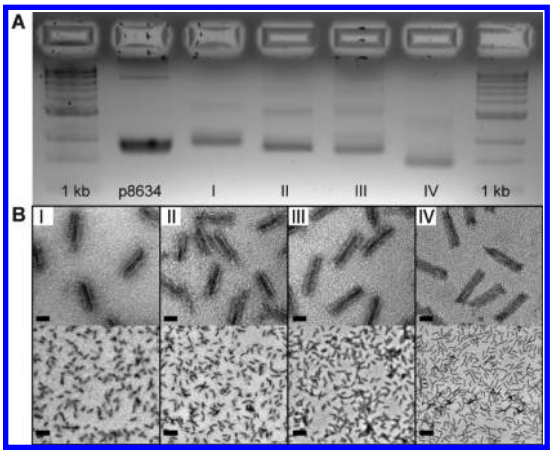

Figure 1. Characterization of DNA origami tubes. (A) Gel analysis of assembled DNA origami tubes after purification with AMICON spin filters. Left to right: 2-log 1 kb DNA ladder, p8634 scaffold, (I) tube CpG, (II) tube CpG PTO, (III) tube chimera, (IV) tube without CpG, 2-log 1 kb DNA ladder. (B) Electron micrograph of the DNA origami tubes I–IV. Scale bars: 30 nm (top), 200 nm (bottom).

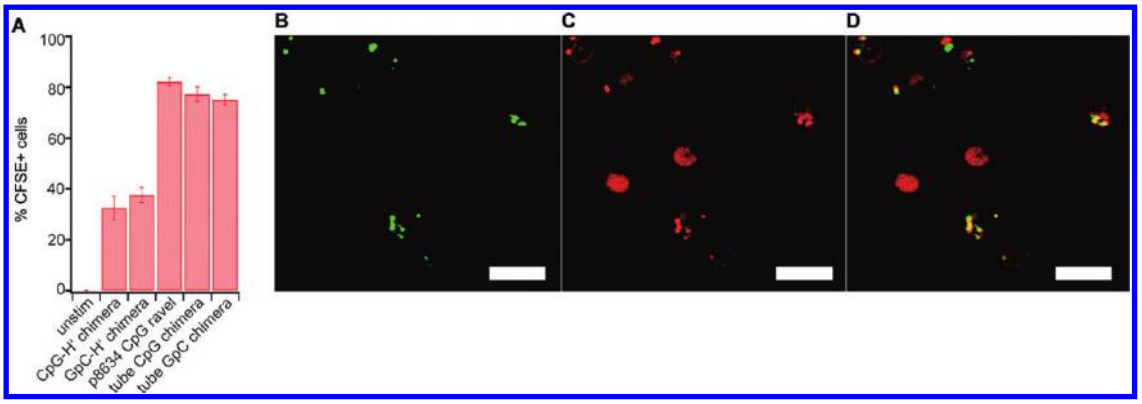

Figure 2. Uptake of CpG-covered DNA nanostructures by immune cells. (A) Uptake of fluorescently labeled CpG sequences coupled to different DNA nanostructures by splenic macrophages. The graph shows the percentage of cells that are positive for the fluorescent marker. Data show the mean value of triplicate samples ± SE and are representative of two independent experiments. (B–D) Confocal micrographs of splenocytes showing intracellular colocalization of DNA origami CpG tubes and lysosomes 4 h after transfection. (B) Green: DNA origami tubes chimera III with FITC. (C) Red: LysoTracker (lysosomes). (D) Merge of A and B. Yellow: colocalized DNA origami CpG tubes in lysosomes. Due to diffusion of cells between time-delayed image capturing of A and B, some colocalized objects are shifted in C. Scale bars: 10 μm.

procedure. The construct has a designed length of ~80 nm and a diameter of ~20 nm, if a spacing of 0.34 nm between two stacking bases and a center-to-center distance of 2.5 nm between two parallel helices is assumed.[5,9] For each of the 62 inner and outer CpG binding sites, a particular staple strand is extended with a 18 nt long sequence H that is complementary to the anchor sequence H′ of the CpG-H′s (Scheme 1). Using the DNA origami tube as a defined carrier of 62 CpG-H′s per structure enables a high local concentration of CpG sequences within the endosomes after internalization. The correct assembly of the DNA structures I–III and the plain tube (IV) was analyzed with gel electrophoresis (Figure 1A) and transmission electron microscopy (TEM) (Figure 1B). The prominent band for all DNA origami tubes as well as the decreased mobility of CpG-decorated tubes (I–III) compared to the tube without CpG (IV) indicates the efficient binding and assembly of the DNA origami tubes.

We first tested whether DNA origami tubes can serve as a delivery tool for immunostimulatory CpG oligonucleotides. Therefore, we analyzed the cellular uptake of fluorescently labeled CpG-H′ strands coupled to different DNA nanostructures (Figure 2A). Freshly isolated mouse splenocytes were incubated with the DNA samples for 3 h, and uptake of fluorescein isothiocyanate (FITC)-coupled CpG-H′ strands was analyzed by flow cytometry. Splenocytes consist of a pool of immune cell subsets, including antigen-presenting cells such as dendritic cells and macrophages that initiate and control immune responses, and immune effector cells such as B and T lymphocytes. The uptake of CpG-H′ strands by macrophages was much more efficient when the CpG oligonucleotides were coupled to the DNA origami tubes or a ravel consisting only of the p8634 scaffold and the handle H′-containing staple strands (p8634 CpG ravel, TEM image in Supporting Figure 6). We conclude that structures of larger size and higher compactness get incorporated more efficiently than individual or short DNA single strands. This effect was independent of the CpG motif as GpC-H′ strands showed similar uptake characteristics. As the receptor that detects CpG sequences, TLR9, is located in the endosome, an endosomal uptake of the DNA origami tubes is a vital prerequisite for the efficient delivery of synthetic TLR9 ligands. Fluorescence microscopy confirmed the colocalization of CpG-decorated origami tubes labeled with FITC together with the endosomal marker LysoTracker, demonstrating that the DNA origami constructs indeed target CpG sequences to the endosome (Figure 2B–D).

To examine whether the DNA constructs induce an immune response, freshly isolated mouse splenocytes were incubated with the DNA samples for 18 h. The immunostimulatory activity of the DNA origami tubes and of all control samples was quantified by measuring the induced secretion of different proinflammatory cytokines such as IL-6 in culture supernatants of stimulated cells by enzyme-linked immunosorbent assay (ELISA). In addition, surface expression of the transmembrane C-type lectin CD69, an early marker of immune activation, was examined on different immune cell subsets by flow cytometry after staining of cell surface molecules by specific fluorochrome-coupled antibodies. The gating strategy for lymphocyte subsets can be found in Supporting Figure 1.

We tested the immunostimulatory activity of the individual components of the DNA constructs, that is, a mix of the 227 staple strands, the p8634 scaffold strand, and the tube without CpG (IV) and observed that the mix of staple strands did not induce detectable IL-6 production. The p8634 scaffold strands and DNA origami tubes without anchors for CpG-H′s induced only low levels of IL-6 (Figure 3). Analysis of further proinflammatory cytokines showed that the release of

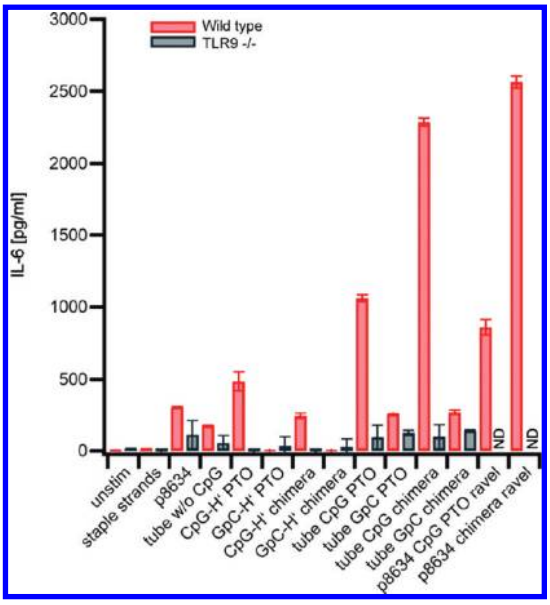

Figure 3. ELISA analysis of IL-6 levels after splenocytes were cultured in the presence of different DNA origami structures for 18 h; 50 μL of 2.4 nM (DNA origami tubes, p8634, staple strands) or 50 μL of 62 $\times$ 2.4 nM (CpG-H′ PTO, CpG-H′ chimera) of sample was added per 400 000 cells in a well. In all experiments, the net CpG weight was 50 ng. Data show the mean value of triplicate samples $\pm$ SE and are representative for two independent experiments.

IL-12p70 in response to the DNA origami tubes was similar to IL-6 (Supporting Figure 2) and that origami tubes did not induce detectable levels of interferon-α or IL-1β (data not shown). Flow cytometry measurements of the early activation marker CD69 on the surface of dendritic cells, a cell type that plays a crucial role in the initiation of immune responses, confirmed these results (Figure 4A). The mix of staple strands did not upregulate CD69 expression, the scaffold strand p8634, as well as the tube without CpG-triggered intermediate cell activation in this cell type. B lymphocytes responded with high expression of CD69 in response to the unfolded p8634 scaffold, while the DNA origami tube induced only moderate CD69 upregulation (Figure 4B,C). The recognition of the DNA origami tube or its individual components was largely independent of TLR9, as cells from mice that are genetically deficient for this receptor (TLR9$-/-$) were activated by these structures to an extent similar to wild-type cells (Figure 4). We thus show that even in the absence of immunostimulatory CpG oligonucleotides, DNA origami constructs can activate innate immunity *via* non-TLR9-mediated pathways, an effect that must be taken into consideration for future applications of DNA origami constructs as drug delivery vehicles.

Next, the ability of DNA origami tubes to act as an efficient nontoxic CpG sequence carrier to induce a potent immune response was tested. The immunostimulation through free CpG-H′s, either with an entire phosphorothioate (PTO) or chimera backbone (Scheme 1), was compared to the immune activation caused by these CpG-H′s bound to the DNA origami tube (Figures 3 and 4). ELISA as well as flow cytometry analysis showed that splenocytes exposed to free CpG-H′s produced moderate amounts of IL-6 and showed intermediate CD69 expression. In contrast, CpG-H′-decorated DNA origami tubes triggered high cytokine production and resulted in an up to 5-fold increase in CD69 expression on splenic dendritic cells. The CpG-induced immunostimulation was entirely dependent on TLR9 since the CpG-mediated increase in immune activation was lost in TLR9-deficient cells. In addition, CpG immune activation was highly sequence-specific, as DNA origami tubes bearing control oligonucleotides with an inverted GpC sequence did not stimulate stronger responses than origami tubes without CpG (Figures 3 and 4). Interestingly, no significant differences in cytokine secretion as well as cell activation was observed for DNA tubes carrying the CpG-H′s on the inner surface or on the outer surface (Supporting Figure 3). This points toward the dissociation of the CpGs from the carrier tubes or toward a partial disassembly of the tubes within the endosome as the TLR9 receptors are embedded in the endosomal membranes and could not access the CpG sequences on the inner surface otherwise.

We further compared the efficacy of the DNA origami tubes for delivery of CpG oligonucleotides to that of the commonly used lipid transfection reagent Lipofectamine, which mediates intracellular delivery of oligonucleotides (Supporting Figure 4).[26] We show that the IL-6 production and CD69 expression on B cells induced by CpG-decorated origami tubes is superior to that induced by the same tubes complexed with Lipofectamine, demonstrating that DNA origami tubes represent an efficient delivery system for CpG oligonucleotides. The cellular viability of cells stimulated with DNA constructs was verified by flow cytometry analysis based on forward and side scattering: The proportion of live lymphocytes did not change following activation with CpG-decorated origami tubes in the absence of a transfection reagent. In contrast, cells incubated with the same tubes complexed with Lipofectamine showed a partly decreased viability (Supporting Figure 5).

Although the amount of CpGs used in all experiments was the same, immunostimulation was strongest when the CpG sequences were conjugated to the carrier tubes. Our experiments also demonstrate that the immune response initiated by the decorated origami tubes does not simply rely on the larger amount of delivered DNA: origami tubes that carry 62 nonstimulating GpC-H′ sequences gave rise to activation levels comparable to tubes without any strands coupled to their anchors (Figures 3 and 4). The highest levels of IL-6 secretion and cell activation were observed for tubes decorated with the chimera CpG-H′s and p8634 CpG ravels, which were not conjugated with

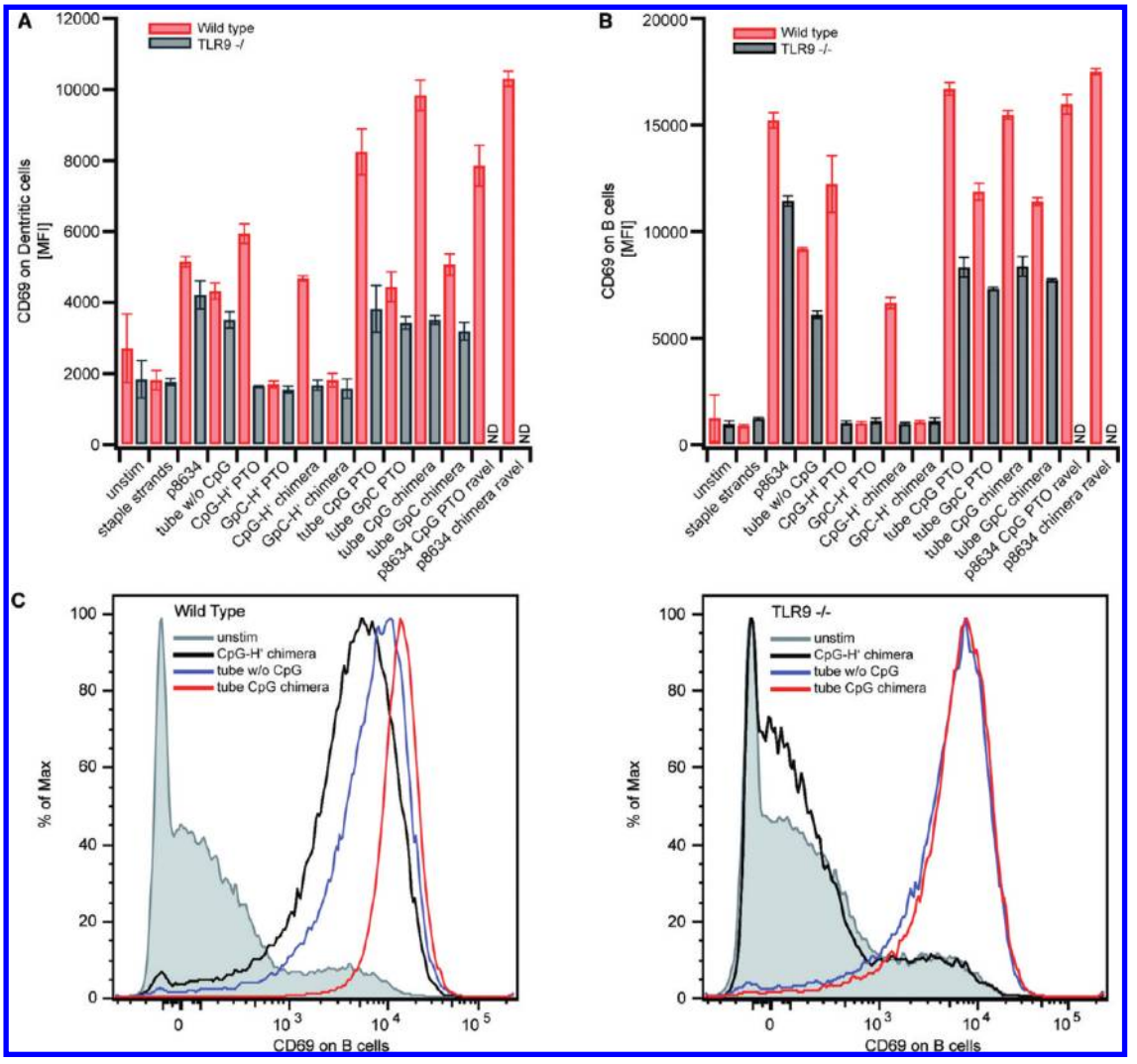

Figure 4. Flow cytometry analysis of immune cell activation after incubation with DNA origami tubes. Freshly isolated splenocytes from wild-type and TLR9-deficient mice were incubated with 50 μL of 2.4 nM (DNA origami tubes, p8634, staple strands) or 50 μL of 62 $\times$ 2.4 nM (CpG-H′ PTO, CpG-H′ chimera) for 18 h. Surface expression of the early activation marker CD69 was analyzed on (A) dendritic cells and (B) B lymphocytes. (C) Representative histograms show CD69 expression on B cells after splenocytes have been incubated for 18 h with the indicated DNA samples. Data show the mean value of triplicate samples $\pm$ SE and are representative of at least two independent experiments. CD69 expression levels are presented as the mean fluorescence intensity (MFI) of the fluorochrome coupled to a specific anti-CD69 antibody.

a transfection agent (Figure 3). This can be explained by the discussed high internalization efficiency of compact and large objects in combination with a degradation-resistant PTO backbone of the conjugated CpGs (*cf.* Figure 2). The slightly less pronounced immune response of cells that were incubated with tubes that carry full PTO-modified CpG-H′s may result from the lower hybridization efficiency of these DNA anchors to their handle sites. This could lead to an untimely dissociation of the CpGs from the carrying tube. Tubes that carry CpG-H′s without any PTO modification also provoke lower immune activation than their chimera-decorated counterparts (Supporting Figure 4), an effect that may originate from the fast degradation of these oligonucleotides in the DNase-rich endosome. Importantly, even CpG oligonucleotides with an unmodified backbone lead to enhanced immune responses when DNA origami tubes are used as carriers, suggesting that this delivery system protects the CpGs to some extent from degradation (Supporting Figure 4B).

We stated above that the elevated immunostimulatory activity of DNA origami structures may result from a more efficient cellular uptake of origami-bound CpG-H′ over free CpG-H′ which might be due to the folded origamis compactness and size. To test this hypothesis, we assembled constructs that consist of the p8634 scaffold strand and only the 62 staple stands that carry the CpG anchors (p8634 CpG ravel). These oligonucleotides are not able to fold the entire scaffold strand and thus form a ravel-like structure with moderate compactness (Supporting Figure 6A). However, CpG-decorated ravels showed similar uptake and activation characteristics as the decorated DNA origami tubes

(Figures 2−4). In contrast, samples that consisted only of the scaffold strand and an excess of CpG oligonucleotides were not able to assemble into any structure and showed low immunogenic potential similar to the scaffold strand alone (data not shown). Our results suggest that the immune-activating potential is not dependent on the three-dimensional (3D) shape but the construct's compactness, size, and stability. Importantly, DNA origami tubes proved to be more stable than DNA ravels when kept in fetal bovine serum (FBS)-containing medium at 37 °C for several hours (Supporting Figure 6B). Uptake studies confirmed this hypothesis by showing less internalization and immune stimulation of DNA ravels compared to origami structures after 4 h of preincubation of the structures in FBS before addition to cells (Supporting Figure 6C). This stability of the DNA origami structure can be an essential advantage that might play a key role in future *in vivo* applications. Further studies on the cell uptake of DNA constructs depending on their 3D shape will help to elucidate this phenomenon.

In conclusion, we describe a novel delivery system for immune-activating CpG oligonucleotides that targets the endosome. This system is built from biomolecules—the origami tube solely consists of DNA—and is nontoxic. The unmodified DNA origami tubes as well as their individual building blocks trigger only non-TLR9-mediated immune responses in primary immune cells. If the same DNA tubes are decorated with CpG sequences, pronounced immunostimulation *via* the TLR9 is observed. Although the biological application of DNA nanostructures is a very young field of research and more studies on the cytotoxicity, the immunological behavior, and the general biocompatibility of DNA constructs must be executed, we believe that such objects can be used as intelligent drug carriers. In addition to being used as enclosing containers that potentially release their payload on demand,[6] DNA architectures can also be modified with biologically active molecules on their surfaces to trigger cellular mechanisms such as immune responses as we have shown in this study. Since DNA oligonucleotides can be modified with a wide variety of biomolecules, this approach could be extended in combination with viral moieties to generate vaccines and adjuvants with nanometer precisely tailored surfaces.

MATERIALS AND METHODS

Design and Preparation of DNA Origami CpG Tube. DNA constructs were designed using the software caDNAno developed by Douglas *et al.*[27] We designed a hollow DNA origami tube with a length of 80 nm and a diameter of 20 nm which can be decorated with up to 62 cytosine-phosphate-guanine (CpG: TCC ATG ACG TTC CTG ACG TT) + anchor sequences (CpG-H′s; H′: AAG ATT ACG GTG AAG AGA) or guanine-phosphate-cytosin (GpC-H′s: TCC ATG AGC TTC CTG AGC TT) + the same anchor sequences. Site-selective binding is achieved *via* the anchor parts H′ of the CpG-H′s that bind to complementary single-stranded DNA handles (H) protruding from the origami structures at defined positions. To achieve an untwisted well-formed DNA origami tube, we chose a honeycomb arrangement of double helices. We used an 8634 nucleotide (nt) M13mp18-based single strand as a scaffold to arrange 227 oligonucleotides (staple strands) into a tube-shaped DNA origami structure consisting of 30 parallel double helices. To prevent stacking effects of blunt dsDNA ends, we connected the ends of two collateral helices with loops of 24−52 unpaired bases. During this study, we used three different types of backbone for the CpG-H′s (5′-TCC ATG ACG TTC CTG ACG TT AAG ATT ACG GTG AAG AGA-3′) to functionalize the DNA origami tube: (I) DNA CpG-H′s consisting of the 20 nt CpG sequence and the 18 nt anchor sequence; (II) CpG-H′s with a phosphorothioate-modified backbone (PTO); (III) chimera CpG-H′s with PTO-modified CpG sequence and unmodified H′ sequence. Those nucleotides also had a fluorescein isothiocyanate (FITC) label on the 5′-end. As a reference, we also prepared a DNA origami tube without conjugated CpG-H′s (sample IV in Figure 1). The staple strands and the unmodified CpG-H′s were HPSF purified by the supplier, and the PTO-modified CpG-H′s were HPLC purified by the supplier. All oligonucleotides were purchased from Eurofins MWG Operon (Ebersberg, Germany). For annealing of the complete constructs, 10 nM of scaffold strand (p8634, M13 mp18 phage-based), 100 nM of each unmodified staple strand, and 12.4 mM of CpG-H′s were mixed in Tris-HCl (10 mM) + EDTA (1 mM, ph 8.0 at 20 °C) and 16 mM $MgCl_2$. This solution was heated to 80 °C for 5 min, cooled to 60 °C over the course of 80 min, and cooled further to 24 °C in 35 min.

Purification of DNA Origami CpG Tube. To remove the 10× excess of staple strands and 20× excess of unbound CpG-H′s after the annealing process, the DNA origami samples were purified using Amicon Ultra-0.5 mL centrifugal filters (100 000 MWCO). Then, 100 μL of annealed DNA origami tubes and 400 μL of buffer (10 mM Tris-HCl + 1 mM EDTA, ph 8.0 at 20 °C + 16 mM $MgCl_2$) were filled into one filter and centrifuged four times at 14 000*g* for 5 min. Between every centrifugation step, the flow-through is removed and the filter is refilled with 500 μL of buffer. To recover the purified DNA origami samples, the filter was turned upside down and centrifuged once more at 1000*g* for 3 min. Overall, roughly 70% of the samples are lost during this purification procedure. We obtained ∼20 μL of 14 nM decorated and undecorated origami samples from each filter.

Gel Electrophoresis and Transmission Electron Microscopy. For analysis of the DNA origami tubes, the samples were electrophoresed in an agarose gel; 2% agarose was dissolved in Tris borate (45 mM) + EDTA (1 mM, pH 8.2 at 20 °C) by heating to boiling. After cooling to 60 °C, $MgCl_2$ (11 mM) was added and filled into the gel cask for solidification. Twenty microliters of 2.4 nM filtered DNA origami tube samples I−IV was each mixed with 4 μL of 6× agarose gel loading buffer (30% glycerol weight-to-volume in water, 0.025% xylene cyanol, 0.025% bromphenol blue) before they were filled into the gel pockets. Additionally, 10 μL of 100 nM scaffold strands (p8634) mixed with 2 μL of 6× agarose gel loading buffer was filled next to the DNA origami tubes as well as a 1 kb 2-log DNA ladder. During running for 3 h at 60 V, the gel cask was cooled in an ice−water bath to prevent heat-induced denaturation of the DNA origami tubes. For imaging, the gel was stained with ethidium bromide (0.5 μg/mL) for 30 min. The filtered DNA origami tubes were further checked by electron microscopy using a JEM-1011 transmission electron microscope (JEOL). The DNA origami structures were adsorbed on plasma-exposed carbon-coated grids (spi Formvar, Cu) and then negatively stained with 1% uranyl acetate for 8 s.

Stimulation of Cells. Female C57BL/6 mice were purchased from Harlan-Winkelmann (Rossdorf, Germany). Mice were 6−10 weeks of age at the onset of experiments. Freshly isolated splenocytes were suspended in ammonium chloride buffer to lyse erythrocytes, washed with PBS, and seeded in a 96-well

plate (Falcon); 400 000 cells per well in culture medium (RPMI VLE, 10% FCS, 2 mmol/L L-glutamine, 100 μg/mL streptomycin, and 1 IU/mL penicillin and 0.0001% β-mercaptoethanol). For stimulation, cells were incubated with different origami probes or oligonucleotides for 18 h at 37 °C in 10% CO_2. For the analysis of origami structure stability, the constructs were kept in serum-containing medium for 4 h at 37 °C prior to cell culture. Culture supernatants and cells were collected and analyzed by ELISA and flow cytometry.

Flow Cytometry and ELISA. Concentration of IL-6 and IL-12p70 in culture supernatants was determined by ELISA according to the manufacturer's instructions (Opteia, BD Biosciences). For flow cytometric analysis, cells were stained with fluorochrome-conjugated monoclonal antibodies (B220, CD3, CD11b, CD11c, CD69, CD80, F4/80, and isotype controls) from BioLegend. For uptake analysis, fluorescence intensity of fluorescein coupled to CpG-H′ was determined by flow cytometry. Data were acquired on a FACSCalibur or a FACSCanto II (BD Biosciences) and analyzed using FlowJo software (Tree Star, Ashland, OR).

Confocal Microscopy. Splenocytes were incubated for 5 h with fluorescein-5′-tagged CpG oligonucleotides, washed, and re-suspended in culture medium. Then, 75 nM LysoTracker (Invitrogen) and 3 μg/mL Hoechst (Invitrogen) were used for lysosomal and nuclear staining. Stained cells were visualized using a confocal laser scanning microscope (TCS SP5II, Leica).

Acknowledgment. We thank J. O. Rädler for helpful discussions. This work was funded by the DFG cluster of excellence Nanosystems Initiative Munich (NIM), DFG LI1743/2-1, and the Bavarian Immunotherapy Network BayImmuNet (to C.B. and S.E.). N.S. and S.H. are supported by the Graduiertenkolleg 1202 of the German Research Foundation.

Supporting Information Available: Additional experimental data, the design and the sequences of the DNA origami construct. This material is available free of charge *via* the Internet at http://pubs.acs.org

REFERENCES AND NOTES

1. Seeman, N. C. Nucleic-Acid Junctions and Lattices. *J. Theor. Biol.* **1982**, *99*, 237–247.
2. Seeman, N. C. Nanomaterials Based on DNA. *Annu. Rev. Biochem.* **2010**, *79*, 65–88.
3. Yurke, B.; Turberfield, A. J.; Mills, A. P.; Simmel, F. C.; Neumann, J. L. A DNA-Fuelled Molecular Machine Made of DNA. *Nature* **2000**, *406*, 605–608.
4. Liedl, T.; Sobey, T. L.; Simmel, F. C. DNA-Based Nanodevices. *Nano Today* **2007**, *2*, 36–41.
5. Rothemund, P. W. K. Folding DNA To Create Nanoscale Shapes and Patterns. *Nature* **2006**, *440*, 297–302.
6. Andersen, E. S.; Dong, M.; Nielsen, M. M.; Jahn, K.; Subramani, R.; Mamdouh, W.; Golas, M. M.; Sander, B.; Stark, H.; Oliveira, C. L. P.; Pedersen, J. S.; Birkedal, V.; Besenbacher, F.; Gothelf, K. V.; Kjems, J. Self-Assembly of a Nanoscale DNA Box with a Controllable Lid. *Nature* **2009**, *459*, 73.
7. Douglas, S. M.; Dietz, H.; Liedl, T.; Högberg, B.; Graf, F.; Shih, W. M. Self-Assembly of DNA into Nanoscale Three-Dimensional Shapes. *Nature* **2009**, *459*, 414–418.
8. Sharma, J.; Chhabra, R.; Andersen, C. S.; Gothelf, K. V.; Yan, H.; Yan, L. Toward Reliable Gold Nanoparticle Patterning on Self-Assembled DNA Nanoscaffold. *J. Am. Chem. Soc.* **2008**, *130*, 7820–7821.
9. Stein, I.; Schüller, V.; Böhm, P.; Tinnefeld, P.; Liedl, T. Single-Molecule FRET Ruler Based on Rigid DNA Origami Blocks. *ChemPhysChem* **2011**, *12*, 689–695.
10. Jahn, K.; Tørring, T.; Voigt, N. V.; Sørensen, R. S.; Kodal, A. L. B; Andersen, E. S.; Gothelf, K. V.; Kjems, J. Functional Patterning of DNA Origami by Parallel Enzymatic Modification of Staple Strands. *Bioconjugate Chem.* **2011**, *22*, 819–823.
11. Schreiber, R.; Kempter, S.; Holler, S.; Schüller, V.; Schiffels, D.; Simmel, S. S.; Nickels, P. C.; Liedl, T. DNA Origami-Templated Growth of Arbitrarily Shaped Metal Nanoparticles. *Small* **2011**, *7*, 1795–1799.
12. Keum, J. W.; Bermudez, H. Enhanced Resistance of DNA Nanostructures. *Chem. Commun.* **2009**, *45*, 7036–7038.
13. Walsh, A. S.; Yin, H.; Erben, C. M.; Wood, M. J. A.; Turberfield, A. J. DNA Cage Delivery to Mammalian Cells. *ACS Nano* **2011**, *5*, 5427–5432.
14. Li, J.; Pei, H.; Zhu, B.; Le Liang,L.; Min Wei, M.; Yao He, Y.; Nan Chen, N.; Di Li, D.; Qing Huang, Q; Fan, C. Self-Assembled Multivalent DNA Nanostructures for Noninvasive Intracellular Delivery of Immunostimulatory CpG Oligonucleotides, *ACS Nano* **2011**, DOI: 10.1021/nn202774x.
15. Nishikawa, M.; Matono, M.; Rattanaki, S.; Matsuoka, N.; Takanura, Y. Enhanced Immunostimulatory Activity of Oligodeoxynucleotides by Y-Shape Formation. *Immunology* **2007**, *124*, 247–255.
16. Ranakiat, S.; Nishikawa, S.; Funabashi, H.; Luo, D.; Takakura, Y. The Assembly of a Short Linear Natural Cytosine-Phosphate-Guanine DNA into Dentritic Structures and Its Effect on Immunostimulatory Activity. *Biomaterials* **2009**, *30*, 5701–5706.
17. Venkataraman, S.; Dirks, R. M.; Ueda, C. T.; Pierce, N. A. Selective Cell Death Mediated by Small Conditional RNAs. *Proc. Natl. Acad. Sci. U.S.A.* **2011**, *107*, 16777–16782.
18. Choi, H. M. T.; Chang, J. Y.; Trinth, L. A.; Padilla, J. E.; Frase, S. E.; Pierce, N. A. Programmable *In Situ* Amplification for Multiplexed Imaging of mRNA Expression. *Nat. Biotechnol.* **2010**, *28*, 1208–1212.
19. Castro, C. E.; Kilchherr, F.; Kim, D. N.; Shiao, E. L.; Wauer, T.; Wortmann, P.; Bathe, M.; Dietz, H. A Primer to Scaffolded DNA Origami. *Nat. Methods* **2011**, *8*, 221–229.
20. Mei, Q.; Wei, X.; Su, F.; Liu, Y.; Youngbull, C.; Johnson, R.; Lindsay, S.; Yan, H.; Meldrum, D. Stability of DNA Origami Nanoarrays in Cell Lysate. *Nano Lett.* **2011**, *11*, 1477–1482.
21. Hemmi, H.; Takeuchi, O.; Kawai, T.; Kaisho, T.; Sato, S.; Sanjo, S.; Matsumoto, M.; Hoshino, K.; Wagner, H.; Takeda, K.; Akira, S. A Toll-like Receptor Recognizes Bacterial DNA. *Nature* **2000**, *408*, 740–745.
22. Hornung, V.; Latz, E. Intracellular DNA Recognition. *Nat. Rev. Immunol.* **2010**, *10*, 123–130.
23. Krieg, A. M.; Yi, A. K.; Matson, S.; Waldschmidt, T. J.; Bishop, G. A.; Teasdale, R.; Koretzky, G. A.; Klinman, D. M. CpG Motifs in Bacterial DNA Trigger Direct B-Cell Activation. *Nature* **1995**, *374*, 546–549.
24. Krieg, A. M. CpG Motifs in Bacterial DNA and Their Immune Effects. *Annu. Rev. Immunol.* **2002**, *20*, 709–760.
25. Ballas, Z. K.; Krieg, A. M.; Warren, T.; Rasmussen, W.; Davis, H. L.; Waldschmidt, M.; Weiner, G. J. Divergent Therapeutic and Immunologic Effects of Oligodeoxynucleotides with Distinct CpG Motifs. *J. Immunol.* **2001**, *167*, 4878–4886.
26. Bourquin, C.; Wurzenberger, C.; Heidegger, S.; Fuchs, S.; Anz, D.; Weigel, S.; Sandholzer., N.; Winter, G.; Coester, C.; Endres, S. Deliver of Immunostimulatory RNA Oligonucleotides by Gelatin Nanoparticle Triggers an Efficient Antitumoral Response. *J. Immunother.* **2010**, *33*, 935–944.
27. Douglas, S. M.; Marblestone, A. H.; Teerapittayanon, S.; Vazquez, A.; Church, G. M.; Shih, W. M. Rapid Prototyping of Three-Dimensional DNA-Origami Shapes with caDNAno. *Nucleic Acids Res.* **2009**, *37*, 5001–5006.